A Framework for a Low Power on Body Real-Time Sensor System Using UHF RFID

Robert Horne and John C. Batchelor, *Senior Member, IEEE*

***Abstract*—This article details the use of an acceleration measuring system which can transmit in real-time sensor data through UHF RFID to a computer. Existing methods of real-time transmission of sensor data rely on power-intensive Bluetooth or Wi-Fi technologies which result in devices that require large bulky batteries, this causes the overall device size to be high and thus can potentially cause issue during use. By harnessing status flags within a specific UHF RFID chip and custom reader software conforming to the EPC GEN2 standard, continuous streaming data rates of 5.2KBps were achievable. These enhanced data rates were shown to be reliable up to a range of 2.4M with above 99.99% data integrity. The power consumption of this methodology was found to be below 2mW during full power continuous transmission. In summary this article outlines and lays the foundation for the use of UHF RFID to deliver sub-2mW low latency, high reliability streaming methods within the domain of on body transmission.**

***Index Terms*—UHF, RFID, accelerometer, low-power, CRFID.**

I. Introduction

THIS use of electronic sensors for the diagnosis and treatment of medical conditions has seen major developments in the last 30 years with innovations such as smartwatches and fitness trackers. Current industry standards revolve primarily around using common wireless communications methods such as Bluetooth Low Energy [1] and WIFI [2], which have been proven sufficient in regard to the transmission of data but are poor when viewed within the power domain. The power domain refers to the usage of a battery within a product, and when the power consumption of a wireless device is high, the current requirements force the size and weight of the design to increase. When focusing on body centric designs, size and weight play a large factor when looking at the ergonomics of the device [3], and whether the device can be correctly mounted and used on the body. The potential applications of body-worn sensors to monitor physical activity and rehabilitation is well recognized, with a number of research groups investigating the optimal sensing platform for objectively detecting the performance of rehabilitation exercises [4], [5]. Some of the known design considerations for these platforms include the need for low power consumption and transmission power [6], a light device that is comfortable to wear that has a low profile [7] and one that is cost effective for successful integration within the U.K.'s NHS (National Health Service) framework [8].

The framework looks to provide a novel low power and efficient communications system for sensors which require low data rate constant transmission (below 5Kbps) and high levels of data integrity within a power domain which can be serviced by very compact thin film batteries or via power harvesting technologies such as passive RF. Passive RF referring to harvesting energy from the reader which is also communicating to the tag in use, or during idle states. One of the lowest power communications methods which is commonly used within industry is Ultra-High Frequency (UHF) Radio Frequency Identification (RFID) [9]. Typical RFID communications are simply requesting an identifier code from a chip for inventory purposes, however more complex chips have been developed by a variety of manufacturers to enable streaming of data through RFID. This functionality allows for the investigation into the streaming of sensors within much lower power domains than that of previous communications technologies as RFID is designed to be passively activated. Some previous investigations have been done into the use of this technology for streaming data [10], however they have not been able to match the transmission performance of conventional technologies. From these previous studies we have been able to isolate a critical area of development which is needed to progress the state of the art to enable high speed transmission, with this area being the ability to synchronize data transmission without the use of handshaking. Synchronization is not usually an issue with the high-power domain systems as they have significantly larger sized packet designs [11], but RFID does not natively have that facility with the EPC GEN2 specification [12].

II. System Design

The system explained in this article can be described in four key areas. Firstly, sensing is the capture of acceleration data. Secondly processing, details the use of a microcontroller to convey and schedule for transmission the data generated in the sensing stage. The communication section outlines the specific way the UHF RFID technique is used to achieve the speeds and reliability needed for streaming the sensor data. Power delivery refers to the procedures used to power and recharge the device, keeping it within the low power domain.

Manuscript received March 5, 2020; revised July 31, 2020; accepted August 4, 2020. Date of publication August 24, 2020; date of current version November 23, 2020. This work was supported by the EPSRC through projects Adaptive Assistive Rehabilitative Technology: Beyond the Clinic under Grant EP/M025543/1 and Formulating and Manufacturing Low Profile Integrated Batteries for Wireless Sensing Labels under Grant EP/R02331X/1. *(Corresponding author: Robert Horne.)*

The authors are with the Department of Engineering and Digital Arts, University of Kent, Canterbury CT2 7NT, U.K. (e-mail: r.j.horne@kent.ac.uk).

Digital Object Identifier 10.1109/JRFID.2020.3018405

A. Sensing

For the framework design used here, a reference from the previous work [13] is taken and the initial system proposed is to stream the data coming from an accelerometer. The accelerometer chosen was the Analog Devices ADXL362 [14]. The accelerometer was used due to its best in class power consumption at time of investigation, ease of use, small form factor and the use of the SPI communications protocol. The low power characteristics of the device allow the accelerometer to consume 270nA during an Idle state and 2 μA at polling rate of 100Hz. A specific feature that aids in the reduction of overall power consumption is an ability for the device to generate an interrupt when it detects movement, thus providing a shake to wake functionality.

B. Processing

The embedded processing is achieved by a Texas Instruments MSP430FR5969 [15]. This microcontroller was chosen for its specific low power features allowing for low current consumption during idle (0.02 μA) and peak (100 μA/MHz) situations. The microcontroller is programmed using Texas Instruments Code Composer Studio. The primary role of the microcontroller in this framework is to act as a data manager between the sensors and the communication side. To ensure timing constraints required to schedule the system an RTOS is employed. This ensures that data polling can be sequenced in accordance with the availability of the memory on the communications stage.

C. Communications

The communications for the circuit are established by an EM Microelectronic EM4325 [16]. Other investigations focus around the streaming of sensor data using other chips such as the AMS SL900A [17] however for this framework the EM4325 was selected due to several critical differences which have allowed faster data transfer rates to be achieved. Firstly, the EM4325 has two stages on internal memory which can be addressed. The standard EERPOM which holds static data such as the EPC TID etc., and a secondary area of 16 Bytes which is Ram Register. The Ram register offering significant read write improvements over the conventional EEPROM memory. The EM4325 also has a battery assisted passive mode which can draw 6 μA to improve read range performance of the device. This reduction in time required to write and then read from memory increases the overall amount of successful read Tag cycles that can occur per second. Secondly, the EM4325 has a feature which allows an external microcontroller to be notified when the chip is being read. This feature allows for communication to occur without the risk of data deadlock occurring due to being confronted with read and write commands at the same time, this is managed by the microcontroller running a statement machine which queues data until such a time that the EM 4325 is not being accessed by the reader. This reduction in deadlock improves the data rate and data integrity.

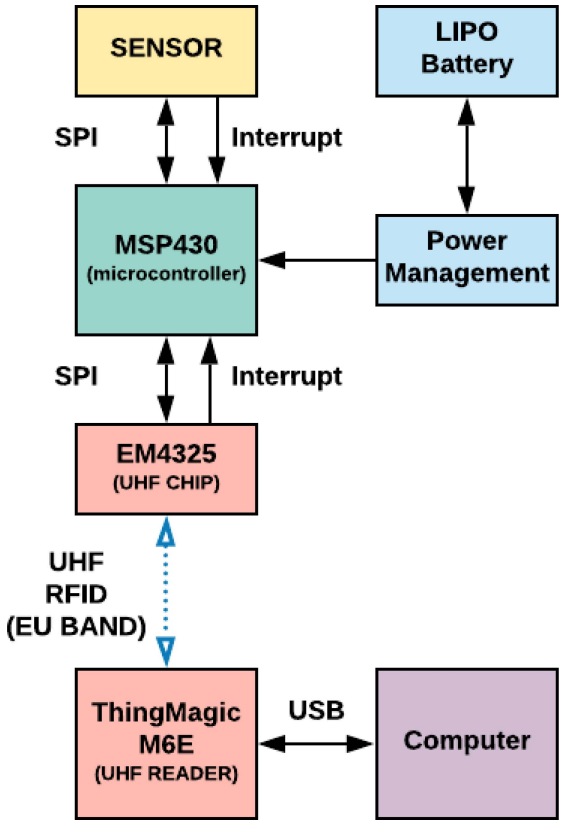

Fig. 1. Entire System Block Diagram.

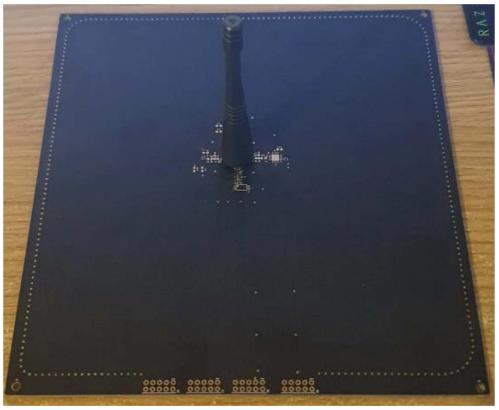

Fig. 2. Dedicated RFID Testing Board with SMA Connector for monopole antenna attachment and large ground plane.

To capture the data being generated by the sensing platform, a Jadak ThingMagic M6E reader [18] was used. To ensure that higher data and integrity rates could be achieved, the Mercury API was used to create a custom C# application. The API allowed for the specific design of an application suited to integration of the device at higher Backscatter frequencies, custom filters, modified hop tables and high-speed polling of the M6E. The reader was not reconfigured outside of the EPC GEN2 specification for the EU Region 2. The reader was attached to a circular polarized antenna with the reader set to 2W EIRP as per the U.K. Ofcom limits [19].

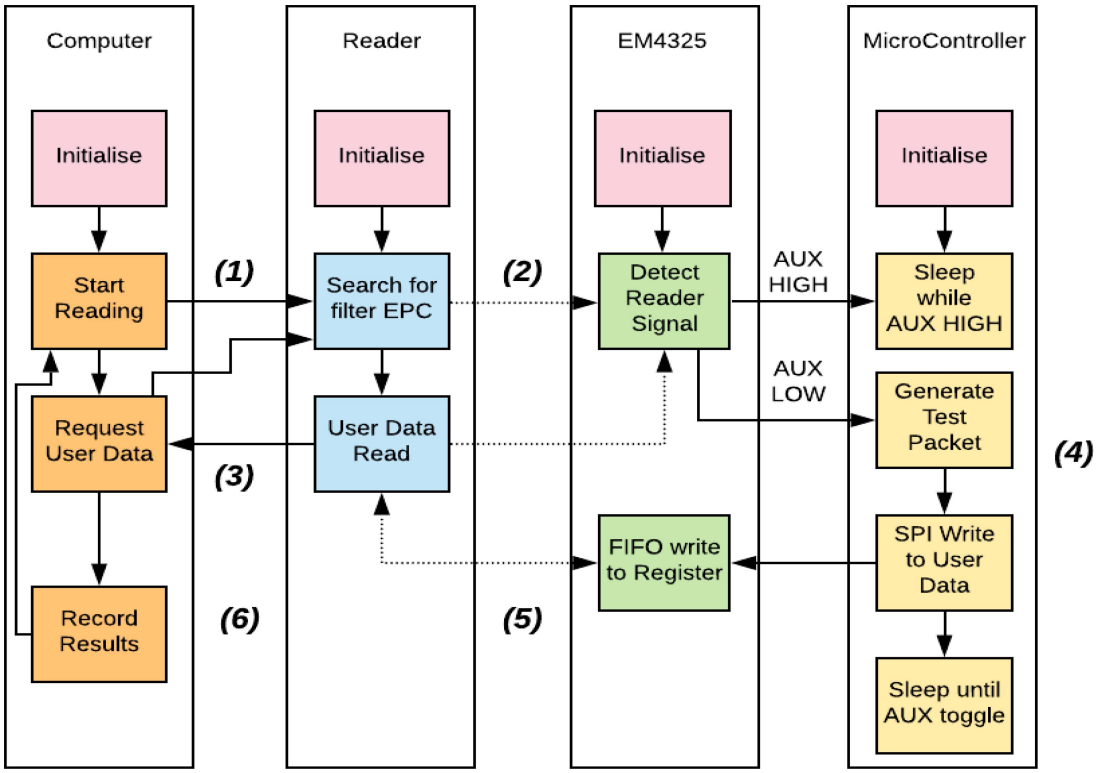

Fig. 3. System State Diagram for a single data transaction.

D. Power Delivery

To deliver a suitable power source to the electronics system, a dual stage power supply was designed. In the first stage was a Lithium Polymer charger which allowed the electronics to interface with standard and custom designed Lithium Polymer batteries rated at between 4.2 and 3.7Vs. The charger would allow a direct discharge into the secondary stage when not in charge mode but would charge the battery when a 5V supply was attached. The secondary stage in the system was a regulator which was needed for the 1.9V supply which was the required voltage rail for the microcontroller, communications and sensing elements.

III. Testing Protocol and Results

A. Synthetic Testing

For the initial testing of the system framework a new dedicated test board was designed and constructed (Fig. 2.) This new design was focused on in air measurements as testing on skin would provide error rates which might not have given good indicators for an initial system design. The board included multiple footprints for common RFID UHF chips including the EM4325.

The EM4325 and antenna board were connected to an MSP430FR5969 development board which ran all of the embedded code. For this testing, no sensors were attached, instead iterating data packets were sent so that packet transmission time and error rates could be easily tracked as any packet which didn't fit the iteration pattern would flag as an error on the computer side (Fig. 3.) To test range, the testing board was moved in stages of 5cm away from the reader. The test was conducted within a shielded room to remove the possibility of external RF noise skewing results.

A high-performance computer was attached to the reader (Intel i9 7960x with 64GB Ram) to remove any latency that could be introduced into the system by slow USB polling, as this had been previously observed with lower specification laptops.

1) Stage One: To begin the computer would establish a serial connection with the reader via USB. Once the connection had been confirmed, settings for reader would be sent detailing the use of Battery Assisted Passive Mode, fast search, Q Factor (0), BSK Frequency(640Khz), Hop table (2 hops) and the polling frequency (Maximum).

The computer would then initiate a start read command using the ThingMagic Mercury API with the specific tag's EPC used as a filter mechanism, this was to ensure good practice in case any other tag infringed on the reading zone. This request is passed via USB Serial to the Jadak ThingMagic M6E. The EPC for the EM4325 had been preprogrammed with a unique identifier for this experiment.

2) Stage Two: The reader would attempt to energize tags within the field, interrogating any tags with the specific EPC filter defined from the computer. This is to ensure the Tag in the experiment is the only tag being engaged during the test, if other tags are within the field during the interrogation, the performance can be degraded. The EM4325 would respond with its EPC and begin to toggle its internal AUX state.

3) Stage Three: Once the reader has established that the desired tag is within the field and able to return an EPC, a further request for Tag Data is sent. This request for data is pointed at the specific register section of the EM4325 for 16 bytes of data. The memory within this area is addressed in

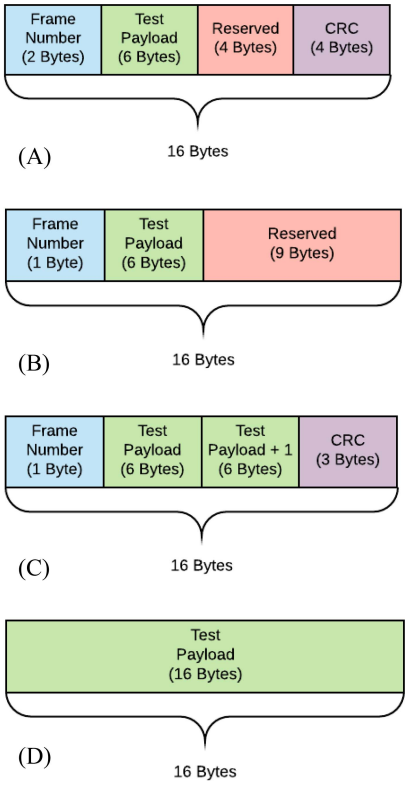

Fig. 4. System Frame Types.

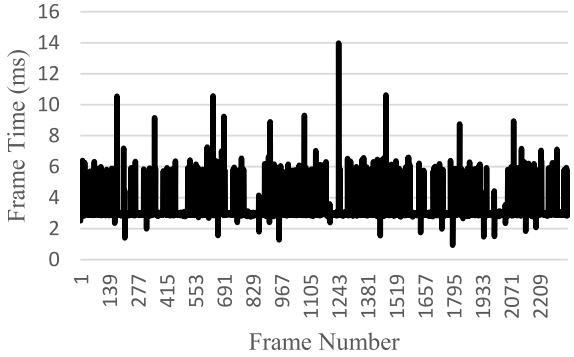

Fig. 5. System Frame Time per transaction.

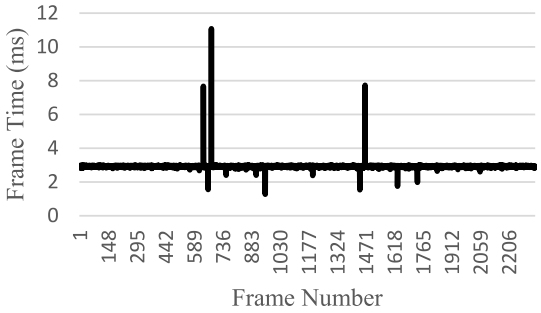

Fig. 6. System Frame Time with packet management per transaction.

logical word addresses, resulting in a query of words 0x104 to 0x10B.

4) Stage Four: As the EM4325 has detected the reader and toggled its AUX pin, the microcontroller can be brought out of a low power idle mode and resumed back to normal operating speed. A test packet is then generated which iterates upon every generation and is transmitted through SPI to the high speed 16 Byte register of the EM4325, this transmission can only occur when the EM4325 AUX pin denotes that the reader is not actively communicating. This technique is used to stop both the microcontroller and the reader accessing the same memory space at the same time, causing a data deadlock. Once this transmission has occurred, the microcontroller can then resume its low power state for conservation of battery power.

5) Stage Five: After the microcontroller has loaded the register, the reader will then read the register, causing the AUX pin to flag that the register is unavailable for the microcontroller.

6) Stage Six: Once the reader has captured the register data, it is then sent back to the computer which can then do a direct comparison with the previous frame of data and check whether the iteration of the frame contents matches. If it did not match, then it would be flagged and would result in an error being presented to the tester, as well as being recorded. The data is logged into a .csv file for further offline processing.

This loop of events would repeat for 3 minutes for differing ranges from the reader and amounts of data read from the frame.

a) Frame layout and design: To send data via the communications line, data needed to be correctly packaged. Within [13] a frame designed for data safety was used (Fig. 4.) (a), as it was only designed to send acceleration data at 60Hz. However, the frame could be reconfigured without certain areas to try and improve performance (b) by only reading 7 Bytes of data.

When analyzing the frame times returned, it can be seen in Fig. 5. that frame times have an average time of roughly 3ms but have constant spikes to 6ms with occasional spikes above 10ms. To mitigate this, double loading of the data from the sensor can be done (c), thus allowing the data to rollover during delayed transmissions (transmissions exceeding 3.5ms).

When using the technique, the frame time stabilizes (Fig. 6.) and only returns spikes for times when the reader is conforming to the EPC GEN2 standard.

Converting the frame to purely iterating data, analysis could be conducted on maximum synthetic performance in terms of both data rate and read range. To generate performance metrics, the system was polled for 30s 5 times for each range and packet size measurement.

Fig. 7. Clearly shows that the performance of the device is providing a steady rate of communication until the testing board is moved to 250 cm away from the reader antenna, whereby the performance indicates that the maximum range has been achieved. The smaller sized packet sizes provide a minor range extension, however they did not provide any viable communication past 265cm. Testing was conducted at 300cm to ensure that a null point was not interfering with the results, but this returned no data transmission from the system. The data integrity rate was observed at 100% until the maximum range of 250cm was reached, beyond that point integrity rapidly decreased.

Within (Fig. 8). we can see a minor decline in update rate when the range is increased, however a minor spike is seen

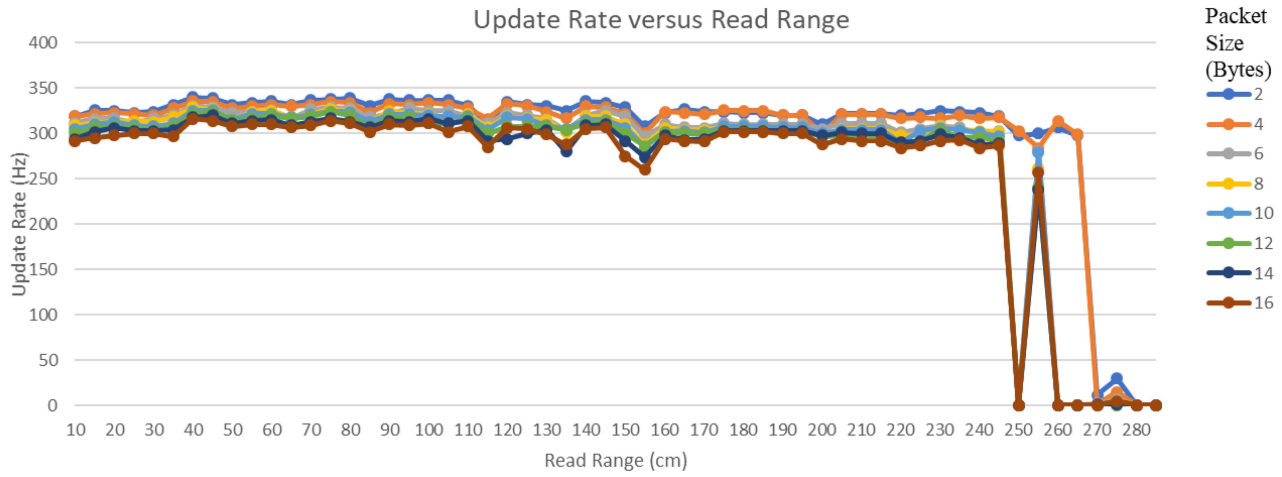

Fig. 7. Update Rate versus Read Range.

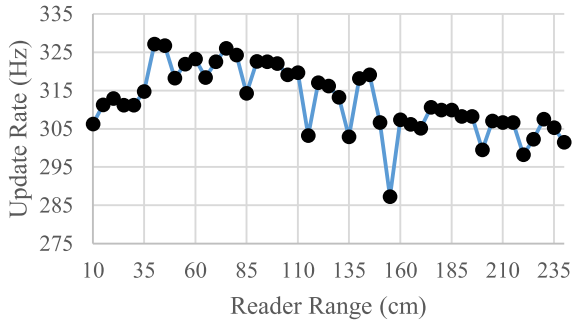

Fig. 8. System Update Rate versus Reader Range.

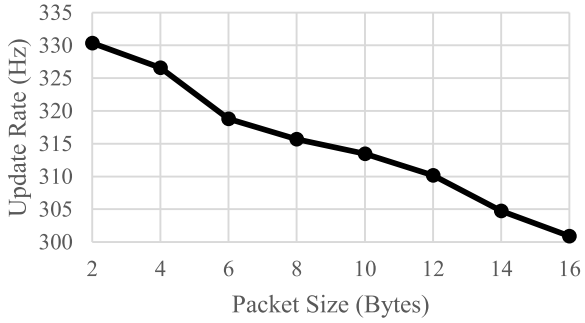

Fig. 9. System Update Rate versus Packet Size.

at the beginning of the measurement, and it is hypothesized that this is due to the reader antenna performing poorly in the near field. It can be argued that the update rate is directly impacted by the packet size by referring to (Fig. 9.) however the difference between smallest and largest sizes results in a drop in frequency of 10% on average. During testing the scheduling system utilizing the auxiliary pin sampling resulted in a 100% data integrity rate.

b) Power consumption: The estimated power consumption for the synthetic test system was calculated to be 775.58 μW, at 408.2 μA (MCU 400 μA) and (EM4325 8.2 μA) at an input voltage of 1.9V. It was assumed that there would be some margin of error in these figures along with losses generated in the regulation phase. Using a calibrated

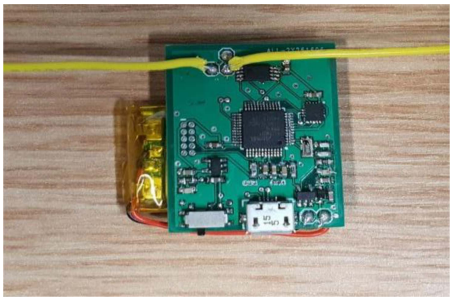

Fig. 10. Acceleration RFID Device.

power source to provide power to the board, the current draw during constant transmission was observed as 619.4 μA at 1.9v thus equaling a power consumption of 1.176mW.

B. Real World Testing

In order to validate the overall performance and reliability of the system, a gold standard inertial tracking sensor system was used in parallel with the framework proposed. The gold standard chosen was the Xsens MVN [20]. This piece of equipment was chosen because of its common use with the academic community, accuracy and its communication methodology, which did not interfere with the framework under test. The devices in use were located on the Right Thigh and Right Shank region. Other locations can be used such as the foot, but for this experiment, only two locations were sampled via the proposed system and the lower body Xsens sensor set was utilized (7 sensors – pelvis and bilateral thigh, shank and feet) to enable comparator sensors for RFID devices placed on the right thigh and shank.

To try to get a reliable correlation between the two systems, the sensor units were placed as close as possible to each other on the body as can be seen in Fig. 11. This allowed for a direct comparison of the data being produced by both sensor units in an offline domain.

To establish a baseline of acceleration performance, five specific movements were chosen:

- KEX – Knee Extension
- KFL – Knee Flexion

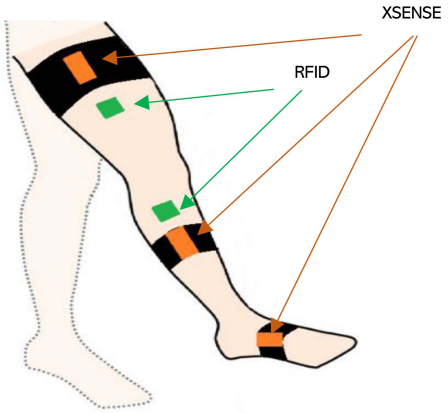

Fig. 11. Sensor locations for both Xsens (Black and Orange) and RFID units (Green).

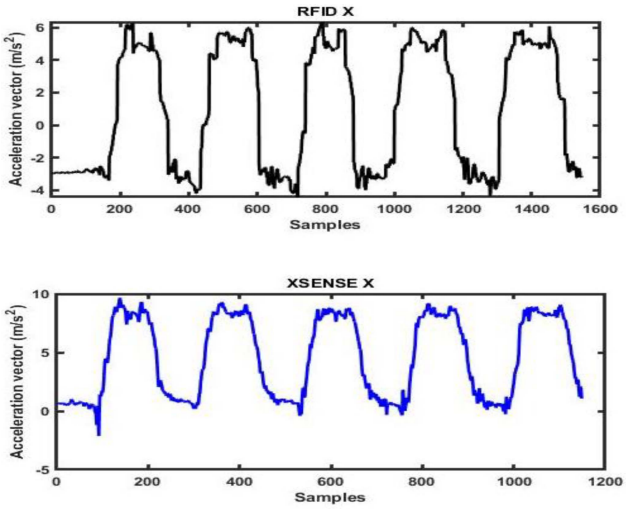

Fig. 12. Accelerometer Data X Axis.

- SLB – Single Leg Balance
- STS – Sit to Stand
- WSH – Weight Shifting

These five early phase knee rehabilitation exercises are included in the Taxonomy for Rehabilitation of knee conditions [21] and are routinely prescribed to those with knee pain or following surgical intentions such as a total knee replacement. Each of the specific actions were repeated 5 times, with 5 repetitions within the action. This resulted in a test data set of 25 unique data samples for each experiment. The experiment was conducted two times, due to requiring both Right Shank and Right Thigh data capture. The UHF RFID reader was placed 1.5 meters from the subject during each test. The range performance of the tag did indicate that more range could be achieved, but a lower value was chosen to ensure the best likelihood of packet integrity. Each of the RFID sensors were attached to plasters using high strength double-sided tape. Both Xsens units were mounted using elasticated straps. To provide an assessment, each of the data sets were compared, looking at the specific graphical signatures produced from each repetition. It was observed that the correlation between the RFID generated and the Xsens Acceleration Vector data was visually high. Giving a clear indication that

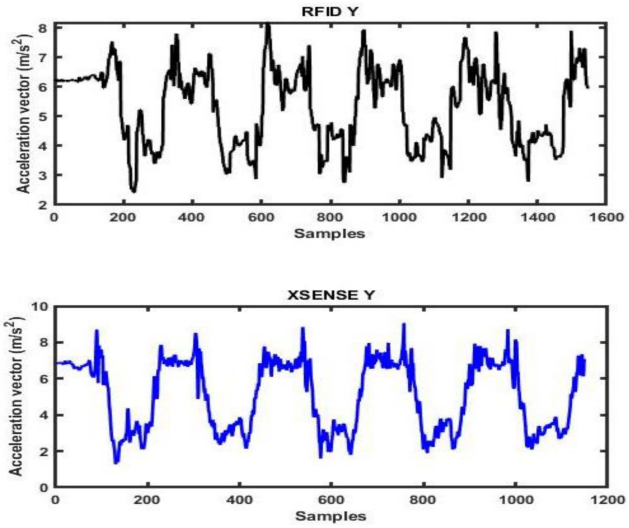

Fig. 13. Accelerometer Data Y Axis.

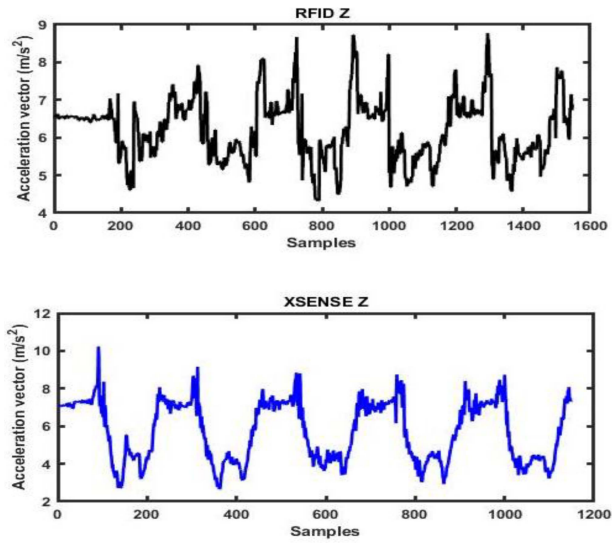

Fig. 14. Accelerometer Data Z Axis.

specific movements, with different acceleration patterns could be isolated from both the RFID and Xsens data set, as well as having a clear correlation between RFID and the Xsens gold standard data.

It can be seen in (Fig. 12, 13, 14) that both systems produce a clear oscillation of five repetitions of a Knee Flexion in respect to acceleration, both having significant visual similarities regarding peaks and troughs. The minor differences seen can be attributed to timing inconstancies on the RFID communications side causing a larger state of change. Nevertheless, each of the five repetitions can be clearly identified. The initial Acceleration vector can also be seen to be different on the two devices, this can be attributed to the sensors having slightly different resting orientations.

IV. Discussion and Conclusion

In conclusion, the article outlines a methodology for using UHF RFID communications to stream sensor data from an

on-body location, at speeds and integrity rates which ensure reliable data analysis can be achieved offline or by supplementary computing power in real-time. The results in both synthetic loading, and real-life scenarios indicated high standards of performance which are comparable to industry standards using more power demanding communication techniques. Furthermore, the article provides techniques which can be employed into different ultra-low power sensing areas for future development, such as EMG and ECG.

The results clearly show that the viability for this technique to be used to stream localized data within a short range from sensors which do not require high levels of bandwidth, can be achieved. Solutions have been provided to deal with EPC GEN2 issues which have arisen, such as random packet fluctuation and reader power down cycling. These software solutions have enabled 3ms latency of packets and 5KBps data transfers rates to be achieved with no impact on the integrity of the data being sent. The software developed can easily be used in commercial and industrial environments due to its conformance with the EPC GEN 2 specification and use of only 2W ERP from the reader.

The power consumption of the synthetic testing proved to be under the predefined limit of 2mW which shows the promise of the system potentially being able to be migrated to a design which is more passively powered in nature. The difference between the estimated and measured results can be concluded as losses in the power regulation phase, which is an area which will require significant investigation in order to achieve higher efficiency.

Further work will take the direction of integrating the device into a flexible printed substrate, which should address issues faced with the scalability of a body centric design. Additional investigations will be conducted into introducing by-directional communications between the systems to allow for configuration of the device during interrogation sessions, as well as development into migrating the design onto an FPGA.

REFERENCES

[1] *Bluetooth Radio Standards 2020*. Accessed: Mar. 1, 2020. [Online]. Available: https://www.bluetooth.com/learn-about-bluetooth/bluetooth-technology/radio-versions/

[2] *IEEE 802.11 Standard 2020*. Accessed: Mar. 1, 2020. [Online]. Available: https://standards.ieee.org/standard/802_11-2016.html

[3] P. S. Taylor and J. C. Batchelor, "Finger-worn UHF far-field RFID tag antenna," *IEEE Antennes Wireless Propag. Lett.*, vol. 18, pp. 2513–2517, 2019.

[4] P. E. Taylor, G. J. M. Almeida, T. Kanade, and J. K. Hodgins, "Classifying human motion quality for knee osteoarthritis using accelerometers," in *Proc. IEEE 32nd Annu. Int. Conf. Eng. Med. Biol. (EMBS)*, Buenos Aires, Argentina, Aug./Sep. 2010, pp. 339–343.

[5] K.-H. Chen, P.-C. Chen, K.-C. Liu, and C.-T. Chan, "Wearable sensor-based rehabilitation exercise assessment for knee osteoarthritis," *Sensors*, vol. 15, pp. 4193–4211, Feb. 2015, doi: 10.3390/s150204193.

[6] H. Alemdar and C. Ersoy, "Wireless sensor networks for healthcare: A survey," *Comput. Netw.*, Vol. 54, no. 15, pp. 2688–2710, 2010.

[7] E. Papi, A. Belsi, and A. H. McGregor, "A knee monitoring device and the preferences of patients living with osteoarthritis: A qualitative study," *BMJ Open*, vol. 5, no. 9, 2015, Art. no. e007980.

[8] E. Papi, G. M. Murtagh, A. H. McGregor, "Wearable technologies in osteoarthritis: A qualitative study of clinicians' preferences," *BMJ Open*, vol. 6, no. 1, 2016, Art. no. e009544, doi: 10.1136/bmjopen-2015-009544.

[9] (2020). *Impinj.com*. Accessed: Jul. 1, 2020. [Online]. Available: https://www.impinj.com/about-rfid/types-of-rfid-systems#:~:text=Ultra%2Dhigh%20frequency%20(UHF)%20RFID,between%20900%20and%20915%20MHz

[10] C. Miozzi, V. Errico, G. Saggio, E. Gruppioni, and G. Marrocco, "UHF RFID-based EMG for prosthetic control: Preliminary results," in *Proc. IEEE Int. Conf. RFID Technol. Appl. (RFID-TA)*, Pisa, Italy, 2019, pp. 310–313, doi: 10.1109/RFID-TA.2019.8891964.

[11] (2020). *Microchipdeveloper.com*. Accessed: Jul. 1, 2020. [Online]. Available: https://microchipdeveloper.com/wireless:ble-link-layer-packet-types

[12] (2020). *GS1*. Accessed: Jul. 1, 2020. [Online]. Available: https://www.gs1.org/sites/default/files/docs/epc/uhfc1g2_2_0_0_standard_20131101.pdf

[13] R. Horne, P. Jones, P. Taylor, J. Batchelor, and C. Holt, "An on body accelerometer system for streaming therapy data using COTS UHF RFID," in *Proc. IEEE Int. Conf. RFID Technol. Appl. (RFID-TA)*, Pisa, Italy, 2019, pp. 301–305.

[14] (2020). *Analog.com*. Accessed: Mar. 1, 2020. [Online]. Available: https://www.analog.com/media/en/technical-documentation/data-sheets/adxl362.pdf

[15] (2020). *Ti.com*. Accessed: Mar. 1, 2020. [Online]. Available: http://www.ti.com/product/MSP430FR5969

[16] (2020). *Emmicroelectronic.com*. Accessed: Mar. 1, 2020. [Online]. Available: https://www.emmicroelectronic.com/sites/default/files/products/datasheets/4325-ds_0.pdf

[17] (2020). *Ams.com*. Accessed: Mar. 1, 2020. [Online]. Available: https://ams.com/sl900a

[18] (2020). *Jadaktech.com*. Accessed: Mar. 1, 2020. [Online]. Available: https://www.jadaktech.com/products/rfid/embedded-uhf-rfid-readers/mercury6e-m6e/

[19] (2020). *Ofcom.org.uk*. Accessed: Jul. 1, 2020. [Online]. Available: https://www.ofcom.org.uk/__data/assets/pdf_file/0025/38095/final_report.pdf

[20] (2020). *Xsens.com*. Accessed: Mar. 1, 2020. [Online]. Available: https://shop.xsens.com/shop/mtw-awinda/mtw-awinda-bundles/mtw-awinda-research-bundle/mtw-awinda-research-bundle-mtw2-dk-2

[21] K. Button, R. W. Van Deursen, L. Soldatova, and I. Spasić, "TRAK ontology: Defining standard care for the rehabilitation of knee conditions," *J. Biomed. Informat.*, vol. 46, no. 4, pp. 615–625, 2013, doi: 10.1016/j.jbi.2013.04.009.

Robert Horne received the M.Eng. (Hons.) and Ph.D. degrees from the University of Kent, Canterbury, U.K., in 2012 and 2017, respectively. In 2016, he joined Evidentia Ltd. as a Research Director, where he worked on embedded skin electronics. In 2017, he became a Research Associate with the School of Engineering and Digital Arts, University of Kent, where he worked on an embedded solution for epidermal ultrahigh-frequency radio frequency identification sensor platform. In 2020, he became a Lecturer in electronic systems with the University of Kent.

John C. Batchelor (Senior Member, IEEE) received the B.Sc. and Ph.D. degrees from the University of Kent, Canterbury, U.K., in 1991 and 1995, respectively. He was a Research Assistant with the Electronics Department, University of Kent, from 1994 to 1996, where he became a Lecturer of electronic engineering in 1997. He currently leads the Antennas Group, University of Kent, where he is also a Professor of antenna technology. His current research interests include ultrahigh-frequency radio frequency identification tag design, passive sensing, body-centric antennas, printed antennas, compact multiband antennas, electromagnetic bandgap structures, and long wavelength frequency-selective surfaces.